Resources, Conservation & Recycling 209 (2024) 107794

Contents lists available at ScienceDirect

Resources, Conservation & Recycling

journal homepage: www.sciencedirect.com/journal/resources-conservation-and-recycling

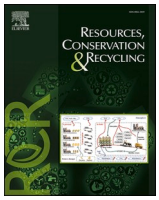

Multiobjective layout optimization for low impact development considering its ecosystem services

Xuanyi Jin [a,b], Delin Fang [a,b,*], Bin Chen [c], Hao Wang [d]

[a] State Key Laboratory of Earth Surface Processes and Resource Ecology, Beijing Normal University, Beijing 100875, PR China
[b] Faculty of Geographical Science, Beijing Normal University, Beijing 100875, PR China
[c] School of Environment, Beijing Normal University, Beijing 100875, PR China
[d] Faculty of Architecture, Civil and Transportation Engineering, Beijing University of Technology, Beijing 100124, PR China

ARTICLE INFO

Keywords:
LID
SWMM
Multiobjective optimization
Ecosystem service value
Optimal layout

ABSTRACT

The augmented proportion of impervious surfaces and heavy rainfall have resulted in waterlogging, nonpoint source pollution, and environmental degradation. Low impact development (LID) is an effective storm management practice. Based on six different LID paving scenarios, a four objective simulation-optimization framework coupled with stormwater management model (SWMM) and NSGA-II that incorporates the ecosystem service value (ESV) was proposed for the optimal layout of LID facilities. A case study in Beijing, China, was taken as an example. The results showed that the rain garden paving scenario is remarkable compared to the other scenarios in realizing ESV, with the dominant ESV of net carbon sinks. The optimization revealed that the change in pollution control rate was more sensitive than the runoff reduction rate. Simultaneously, the optimization of these two indicators will be accompanied by more cost and lower ESV. The optimal solution achieved 32.48 % of runoff reduction rate, 82.22 % of water pollution control rate, 0.73×10^5 CNY of ESV, and 2.29×10^6 CNY of cost. The framework provides reference and technical support to achieve the synergistic objectives among cost, water quality and quantity control, and ecosystem services.

1. Introduction

Rapid urbanization expands impervious subsurface, enhancing surface runoff and thus exacerbating the risk of waterlogging (Shafique and Kim, 2017; Song et al., 2018; Zhai et al., 2021). Climate change increasingly intensifies the severity and frequency of damage by affecting precipitation (Heidari et al., 2023; Yu et al., 2022). Furthermore, in stormwater runoff, most pollutants are carried into urban water bodies, triggering problems such as pollution originating from decent water sources (Hashemi and Mahjouri, 2022; Rezaei et al., 2021). Low impact development (LID) facilities cope with these basic problems, concomitant with various ecosystem service values (ESV) (Zhang et al., 2018). While achieving these objectives simultaneously is challenging, trade-offs should be considered when evaluating multiple objectives and LID facility configurations.

LID is an emerging stormwater management practice (Chuang et al., 2023) that focuses on regulating stormwater runoff and managing nonpoint source pollution, intending to control runoff at its origin. It aims to minimize disruption to the natural environment during construction, thereby facilitating the natural return of runoff to the hydrological cycle (Darnthamrongkul and Mozingo, 2021). Representative practices of LID include green roofs, rain gardens, permeable pavements, and vegetation swales (Eckart et al., 2017). Recent studies have proven that these LID facilities are efficient across many dimensions, containing reduced surface runoff, mitigated stormwater pollution, and a series of ESV like recreation and education (Liu et al., 2022; Toledo-Gallegos et al., 2022; Wang, R. et al., 2022). The application of LID elements to a diverse range of project types and locations is now indisputably recognized as a catalyst for advancing the sustainable development of urban areas. Applying LID elements at a smaller scale, for instance, scaling down to block or neighborhood units, allows for a subtler consideration of diverse facility characteristics, providing insights and strategies for broader implementation (Luo et al., 2023).

Communities account for a significant proportion of urban built-up land. The application of LID facilities in communities helps to identify the impact of specific factors such as precipitation and topography (Ghodsi et al., 2020). Smaller scale domains as communities combined with higher-resolution elevation data can result in more refined

* Correspondence author at: No. 19, Xinjiekouwai St., Beijing 100875, PR China.
E-mail address: fangd@bnu.edu.cn (D. Fang).

https://doi.org/10.1016/j.resconrec.2024.107794
Received 30 January 2024; Received in revised form 23 June 2024; Accepted 25 June 2024
Available online 2 July 2024

modeling, thus helping communities visualize actual runoff conditions and obtain more accurate simulation results (Hou et al., 2021; Yin et al., 2020). In addition, the planning process can incorporate community priorities for differentiation (Reckner and Tien, 2023). Representative sponge communities at home and abroad include the High Point Residential LID project in Seattle, USA, and the LID system construction project in Shenzhen Guangming new district (Sun, 2020). These communities improve access to green space in social housing contexts by combining LID facilities and landscape gardening design to manage rainwater and flooding adequately (Truong et al., 2022) and improve the living environment of residents. The development of multifunctional LID facilities contributes to community adaptation and ideal development pathways to guide wider urban transformation (Lovell and Taylor, 2013). Particularly, Beijing has suffered severe waterlogging due to the extremely heavy rainfall in 2012, which resulted in substantial casualties and economic losses. As urban waterlogging is likely to worsen in the future (Ji et al., 2024) and the further spread of NPS triggered by waterlogging, residential areas also tend to contribute more NPS pollutants than roads (Zhi et al., 2018). It was shown that regulating NPS sources through LID is important in controlling pollutants such as COD and building a quality water environment (Ji et al., 2022). Therefore, this study with the community as the study area can build on the characteristics of the area and give a more scientific and appropriate option for the laying of LID facilities.

One of the models that include methods capable of simulating the operation of the LID facility performance is the stormwater management model (SWMM) from Environmental Protection Agency (EPA) (Alamdari and Sample, 2019), which has been predominantly used by many scholars. It was found that the model is very effective in simulating urban storm flooding, designing drainage network systems, estimating urban nonpoint source loads, and assessing the risk of waterlogging (Liao et al., 2015; Qin et al., 2013). It can also simulate the water quality and quantity of runoff generated from sub-basins at any point at different time-step intervals under a given rainfall scenario and the flow and depth of water in each pipe and channel (Huang et al., 2018). Changes in rainfall may negatively impact drainage systems and even lead to infrastructure failure (Rong et al., 2024). Therefore, it is necessary to compare the differences in LID effectiveness across different return periods. However, when setting up the practicalities of LID facility planning, the best LID combination performance is often difficult to uncover due to the density and complexity of the subcatchments (Rezaei et al., 2021).

To enable the achievement of an integrated trade-off between the different objectives, optimization tools play a crucial role in efficiently evaluating and comparing LID paving scenarios (Eckart et al., 2018). Multiobjective optimization is more commonly applied than single objective optimization as it eliminates the need for preference selection before decision-making (She et al., 2021). When faced with different LID installation scenarios, it is possible to minimize stormwater runoff, reduce costs and inputs, etc., within the constraints (Hou et al., 2020; Rezaei et al., 2021). The combination of multiobjective optimization with SWMM has become the trend of LID layout optimization (Zhu et al., 2023). Multiobjective optimization covers several classifications such as traditional methods and intelligent algorithms. Weighted and goal programming algorithms traditionally belong to the traditional approach, which tends to convert multiple objectives into a single objective for an optimum solution. Gao et al. (2021) used the technique for order preference by similarity to ideal solution (TOPSIS) to select the best LID facilities combination based on the simulation by SWMM. Koc et al. (2021) obtained the optimal selection of LID scenarios based on 16 sustainable development-related indicators, incorporating the analytical hierarchy process and TOPSIS methods. In comparison, genetic algorithms, particle swarm optimization, simulated annealing algorithm, etc. are intelligent algorithms, which can search for possible objective solutions simultaneously and finally form an optimal solution set (Huang et al., 2018; Minh Hai, 2020; Shojaeizadeh et al., 2021; Yu et al., 2022). Among these intelligent algorithms, the Non-dominated Sorting Genetic Algorithm (NSGA-II) has a final solution set with relatively good convergence and enlarges the sampling space to avoid losing the best individuals. The optimal deployment scheme of NSGA-II and SWMM for joint solution of LID can be applicable. Alamdari and Sample (2019) coupled SWMM and NSGA-II for optimal objectives such as cost, runoff, and pollutant reduction. However, most studies on coupled stormwater modeling and optimization algorithms focus on regular objectives, with more attention paid to refined combinations of cost, water quantity reduction, and water quality pollution control as the main objectives. For a more explicit presentation of the trade-offs between ESV and cost, the two are not combined into a single objective in this paper. Considering the significance of synergizing the ESV of LID facilities with other conventional objectives, there is an urgent need for a more integrated optimization framework to address the optimal layout of LID facilities.

In addition to mitigating the risk of waterlogging and pollution, LID facilities are accompanied by a range of extra ESV that are the benefits that humans derive from ecosystems (Behboudian et al., 2021; Toledo-Gallegos et al., 2022). Since pollution, flooding, and many other problems are often due to the failure to consider ESV and their internal interactions, it is essential to consider ESV in urban planning (Behboudian et al., 2021). It was found that scientific configuration of LID facilities and neighborhood improvements are successful for a wide range of ESV (Wang, W. et al., 2022). Combining the characteristics of different LID facilities, such as permeability, vegetative cover, rainwater harvesting, etc., and evaluating their utilities can promote the solution of funding issues through value revelation (Van Oijstaeijen et al., 2023). Many scholars have developed assessment frameworks to account for the value of ecosystem services in regional scenarios, like climate regulation(Ashrafi et al., 2022), carbon sink (Heusinger and Weber, 2017), and so on. However, current studies estimate these values mostly from an evaluation perspective and ignoring the overall benefits of paving multiple LID facilities. The mainstreaming of comprehensive valuations for greening practices potentially reinforces the argument for the green option (Van Oijstaeijen et al., 2023). Based on a more comprehensive analytical framework for LID facilities, community residents tend to derive benefits from their surroundings and enhance their sense of well-being. In addition, policymakers and urban planners can obtain sufficient evidence to formulate urban development plans that consider green and multifunctional aspects (Korkou et al., 2023).

This research proposed an innovative multiobjective optimization framework considering ESV for the layout of LID facilities. On the one hand, six deterministic scenarios were constructed based on the selection of four types of LID facilities. The performances of scenarios were comprehensively analyzed given runoff reduction rate (RRR), pollution control rate (PCR), cost, and ESV. On the other hand, the research coupled the SWMM with the NSGA-II to achieve the multiobjective optimization layout of LID facilities. The research selected a neighborhood in Beijing as a case study.

2. Methods

Figure S1 shows the methodology flowchart. First, the SWMM model was established based on parametric and rainfall pattern design. Second, four LID facilities were selected to design six deterministic scenarios. Four objective functions, i.e., runoff reduction rate, water quality pollution control rate, cost, and ESV, were also established. The values for the objective functions were also calculated for different deterministic scenarios under storms with different return periods. Finally, the SWMM and NSGA-II were coupled to obtain the optimal configuration results of LID facilities.

2.1. Study area

The study area is located in Beijing, China. The neighborhood is a residential site covering an area of 11.80 hectares (Fig. 1). It experiences

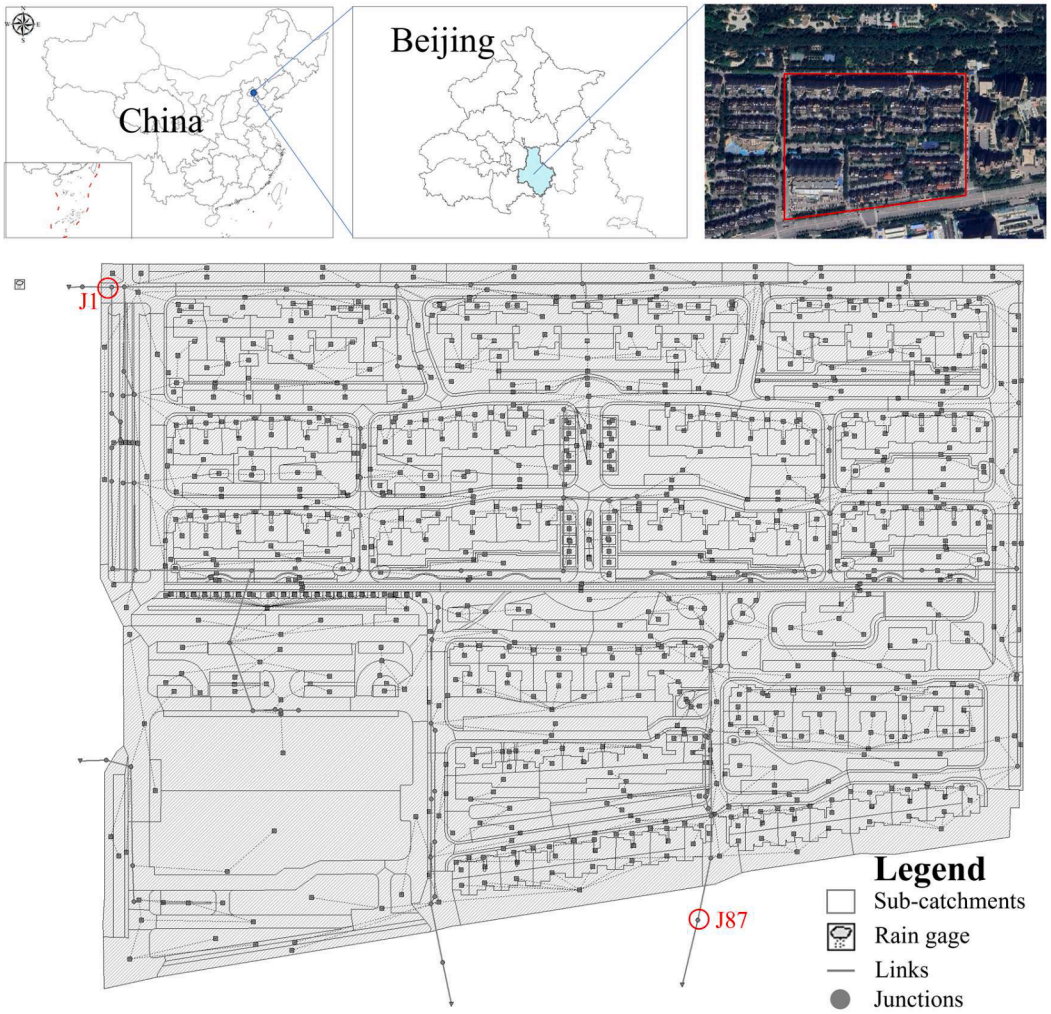

Fig. 1. Location of the study area and SWMM generalization.

a temperate monsoon climate with distinct seasons. Summers are hot and rainy, while winters are cold and dry. The overall terrain slopes relatively gently, with slopes in the district's northern, southern, and central parts, where the average slope is 1.39 %. The original area was not paved with LID facilities that could be broadly categorized into three types of subsurfaces: roads, roofs, and green spaces, the roughness coefficients of which are 0.02, 0.02, and 0.2 respectively (Fig. S2). Considering the predominance of impervious surfaces and the fact that green spaces are mostly flush with the road surface, the level of waterlogging control during rainfall in the study area needs to be improved. Therefore, the study area is expected to implement four types of LID measures: green roof (GR), vegetation swale (VS), rain garden (RG), and permeable paving (PP).

2.2. Design rainfall

The rainfall was designed following the Beijing storm intensity formula to simulate rainfall events under different return periods (Fig. S3):

$$q = \frac{2001(1 + 0.811lgP)}{(t+8)^{0.711}} \quad (1)$$

where q is the intensity of the storm design [liters/(s*ha)], t is the rainfall duration (minutes), and P is the return period (years). The scope of the application is $t \leq 120$ min and $P \leq 10$ years.

$$q = \frac{1378(1 + 1.047lgP)}{(t+8)^{0.642}} \quad (2)$$

where the scope of the application is $t \leq 120$ min and $P > 10$ years.

On the basic Chicago rainfall rain pattern design, rain peak is 0.4 to design the return period P. In this study, the 2-h short-calendar time design rainfall pattern is used to establish the rainfall time series of 1a, 5a, 10a, 20a, 50a, and 100a, which also serve as inputs to the subsequent rainfall amounts under various design scenarios.

2.3. Storm water management model

2.3.1. Model description

SWMM, developed by the US EPA in the 1970s, is a dynamic rainfall runoff simulation tool that simulates urban storm flooding, designs drainage network systems, estimates urban nonpoint source loads, and assesses flooding risk (Huber et al., 1988; Yang et al., 2023). The SWMM can be used to divide the catchment into smaller subcatchments. Based on the network of pipes within the catchment, flow paths can be formed to connect the subcatchments. Taking into account infiltration, evapotranspiration, and depression storage, each subcatchment is affected by upstream pollutants in addition to stormwater pollution (Eskandaripour et al., 2023). In particular, the current version of SWMM allows for the direct setup of LID facilities, with the LID module consisting of three layers, i.e., surface, soil, and drainage mat (Hamouz and Muthanna, 2019).

2.3.2. Establishment of SWMM

The basic data needed for this study include land cover data, DEM data, drainage data, and so on. To construct a comprehensive model of the drainage system, it is necessary to gather precise data about the fundamental physical and geometric parameters of the pipes. Furthermore, a thorough understanding of the spatial topology of the pipe network is indispensable for completing the entire model. The principles of Tyson polygons were used to divide the area based on pipe node distribution through ArcGIS software. A total of 930 subcatchments, 86 stormwater wells, 2.2 km of stormwater pipelines, and 4 outfalls were obtained after model generalization of the study area.

The main parameters in the catchment include infiltration model, width, percentage of slope, (un)permeable Manning's N-value, and percentage of (un)permeable depression storage and no depression storage. In this case, the infiltration model represents the infiltration curve, while the width represents the characteristic length of surface diffuse flow (Table S2). Since there was a lack of empirical data in this study, the validity of the parameter settings was maintained by keeping the continuity error within 10 % at each simulation. The results show that the SWMM parameters are feasible to choose.

Due to the lack of basic monitoring conditions in the residential area, this study selects the values of each parameter cautiously based on the engineering investigation report of the project, the SWMM user manual (Huber and Dickinson, 1988), and relevant research literature (Zhang, 2012). The study strictly controls the continuity errors in the subsequent simulations. The water quality parameters include the cumulative modeling parameters of surface pollutants in different subsurfaces and the pollutant flushing parameters (Tables S3 and S4).

2.3.3. Model validation

The Nash–Sutcliffe efficiency (NSE) in Eq. (3) was used in the research for parameter validation of the establishment of SWMM (Nash and Sutcliffe, 1970). The NSE indicates the degree of fit between observed data and simulated results, with a higher value closer to 1 representing a better fit.

$$NSE = 1 - \frac{\sum_{t=0}^{T}\left(Q_{measure}^{t} - Q_{simulate}^{t}\right)^2}{\sum_{t=0}^{T}\left(Q_{measure}^{t} - \overline{Q_{measure}}\right)^2} \tag{3}$$

where $Q_{measure}^{t}$ is the measured depth of observed inspection well at time t, $Q_{simulate}^{t}$ is the simulated depth of observed inspection well at time t, and $\overline{Q_{measure}}$ is the mean value of all measured depths of observed inspection wells.

The depth of waterlogging of two inspection wells J1 and J87 are recorded. The rainfall event 2021–7–18 with a rainfall amount of 12.8 mm was used, the rainfall duration of which is 720 min. The rainfall event 2022–7–22 with a rainfall amount of 64.8 mm and duration of 600 min was also used. Figure S4 shows the records of measured and simulated results. The NSE for model validation are 0.902 and 0.888 in rainfall event 2021–7–18 for J1 and J87 and 0.880 and 0.877 in rainfall event 2022–7–22 for J1 and J87, respectively.

2.3.4. Scenarios design and simulation

Based on the distribution of buildings in the study area, four types of LID facilities are used in this study: PP, VS, RG, and GR. PP can be installed on road surfaces, VS and RG can be arranged on green spaces, and GR can be installed on roofs. Only one type of LID facility will be installed in each subcatchment to ensure that the facilities are effective and continuous with each other. Six deterministic scenarios are designed for exploring the mechanisms of how different LID facilities function. The deterministic scenarios include a baseline scenario that paved with no LID facilities, four single type of LID paving scenarios, and an integrated adjusted scenario that paved with four types of LID facilities.

The paving principles generally followed the applicability of LID facilities that are illustrated in detail in the appendix S1.

The study area was designed with six paving options corresponding to different scenarios in Table 1. The distribution for Scenario F was presented in the appendix (Fig. S5).

2.4. Multiobjective coupled optimization model

2.4.1. Objective functions

2.4.1.1. Runoff reduction rate

$$RRR_Z^i = \frac{R^i - R_Z}{R^i} \tag{4}$$

where RRR_Z^i is the runoff reduction rate under the Zth LID facility deterministic scenario in the ith return period, R_Z is the surface runoff under the Zth LID facility construction scenario that can be acquired from SWMM, and R^i is the rainfall for ith return period.

2.4.1.2. Runoff pollution control rate

$$PCR_Z^i = \frac{PC_A^i - PC_Z^i}{PC_Z^i} \tag{5}$$

where PCR_Z^i is the runoff pollution control rate under the Zth LID facility deterministic scenario in the ith return period, PC_A^i is the surface pollutant load under the baseline scenario, and PC_Z^i is the pollutant load under Zth scenario, such as COD_Z^i, TP_Z^i, TN_Z^i, or the sum of the three. The pollutant load can be obtained from the simulation of SWMM.

2.4.1.3. Cost. Investing and constructing LID facilities involves two main types of costs: one-time investment costs during the construction phase and ongoing management and maintenance costs during the subsequent maintenance phase. This study compiled a cost list based on the standard for sponge city of construction and design (Ministry of Housing and Urban-Rural Development, 2018), assuming a maintenance period of 30 years (Table S5).

$$Cost_Z = \sum_{m=1}^{k_Z}\left(a_m - \frac{1-(1+DR)^{Y-1}}{Y} * b_m\right) * S_Z \tag{6}$$

where $Cost_Z$ represents the total economic cost under Zth deterministic scenario, CNY; m represents the type of LID, $m = 1$ represents PP, $m = 2$ represents VS, $m = 3$ represents RG, and $m = 4$ represents GR; a_m represents the construction cost per unit area of a LID facility, CNY/m^2; b_m represents the maintenance cost per unit area of a LID facility, CNY/m^2; Y represents the maintenance year as 30; k_Z represents the number of subcatchments under Zth deterministic scenario; DR represents discount rate, which is also known as the real-time interest rate (3.5 % in this study); k_Z represents the number of subcatchments under the Zth scenario; and S_Z represents the total area occupied by the Zth scenario, m^2.

2.4.1.4. Ecosystem service value.

(1) Net Carbon Sink

Carbon emissions from LID facilities need to be accounted for in

Table 1
Six deterministic scenarios.

Scenarios	LID facilities paving type and area
A	No LID facilities
B	GR (7055.46 m^2)
C	VS (13,336.22 m^2)
D	RG (13,336.22 m^2)
E	PP (89,300.09 m^2)
F	GR (7055.46 m^2) + VS (11,341.28 m^2) + RG (1994.94 m^2) + PP (89,300.09 m^2)

relation to the processes that generate carbon emissions over the entire life cycle of the facility, such as the production of building materials, transportation of building materials, construction activities, and operation and maintenance. The first three components are one-time carbon emissions, while operation and maintenance require interannual repetition in the calculation. The specific calculation is shown below.

The composition of different types of LID facilities and the one-time carbon emission inventory table mainly refer to (Li et al., 2019):

$$CE_Z^O = CE_m^O * S_Z \tag{7}$$

where CE_Z^O represents the total one-time carbon emissions of the Zth deterministic scenarios, kg CO_2; CE_m^O represents the total one-time carbon emissions of mth type of LID, kg CO_2/m^2; and O represents the one-time and NO represents the nonone-time.

$$CE_Z^{NO} = CE_m^{NO} * Y * S_Z \tag{8}$$

where CE_Z^{NO} represents the non-one-time carbon emissions of the Zth deterministic scenarios, kg CO_2 and CE_m^{NO} represents the total non-one-time carbon emissions of mth type of LID, kg $CO_2/(y*m^2)$.

The carbon sink capacity of LID facilities is mainly divided into two parts. First, GR and RG can directly sequester carbon by using the ability of plants to fix carbon dioxide. Second, since all LID facilities can store rainwater and provide processed wastewater, the carbon emissions generated during the treatment and transportation of this water are correspondingly reduced. The difference in carbon sink between PP and VS is mainly evident in the latter

$$CS_Z^D = \sum_{m=1}^{m=k_Z} X * S_Z^V * 2k_Z \geq m \tag{9}$$

CS_Z^D is the direct carbon sink of LID facilities in the Zth scenario; X is the average annual carbon sink from CO_2 uptake by leaf photosynthesis, taken as 13.63 $kgCO_2/(y*m^2)$ (Li et al., 2019); and S_Z^V represents the area that possesses vegetation under the Zth scenario. Set 2 years for plants to reach the maximum value of carbon storage.

The volumetric method is used for calculating carbon emission reductions due to reduced water consumption.

$$CS_Z^I = V_m * 1.07 * S_Z \tag{10}$$

CS_Z^I is the indirect carbon sink of the ith LID facility in a given area and V_m is the volume that can be controlled by the mth LID facility per m^3 for a given storm intensity, the value of which can be evaluated by the structure of the facility. The height of the berm referred from engineering file, with 100 mm for GR, 100 mm for VS, 65 mm for PP, and 100 mm for RG. Then, 1.07 is the amount of carbon emissions that can be reduced for every 1 m^3 of rainwater reused.

In summary, the benefits of net carbon sink can be expressed as follows:

$$NCS_Z = C_{Price} * \left[\left(CS_Z^D + CS_Z^I\right) - \left(CE_Z^O + CE_Z^{NO}\right)\right] \tag{11}$$

where C_{Price} represents the carbon tax price set at 60 CNY/t (Huang et al., 2023). The value of the net carbon sink is based on carbon emissions (one-time and non-one-time) and carbon sinks (direct and indirect). Calculations are made using the net carbon sinks during the operational period and the carbon price in the beginning year.

(2) Temperature Regulation

The value of temperature regulation is mainly reflected in the value of reducing electricity consumption through heat evaporation. Therefore, LID facilities can reduce temperatures, increase humidity, and regulate the climate of localized areas by absorbing heat through evaporation of water.

$$TR_Z = \frac{q_Z^h * E_{Price} * \gamma}{3600 * \alpha} + \beta * q_Z^h * E_{Price} \tag{12}$$

$$q_Z^h = \frac{ET * S_Z^W}{10^5} \tag{13}$$

where TR_Z represents the temperature regulation value of the Zth scenario. q_Z^h is the annual evaporation loss under the Zth scenario. E_{Price} is the standard electricity price in Beijing, taken as 0.488 CNY/(kW·h) (Deng et al., 2019). α is the energy efficiency ratio of the air conditioner, taken as 3; γ is the heat of vaporization at one standard atmosphere, taken as 2.26×10^6 J/kg; β is the power consumption for converting water under $1m^3$ into steam, taken as 125 kW·h (Zhang et al., 2021). ET is the annual evapotranspiration, the data of which was obtained from the Beijing Water Resources Bulletin. S_Z^W is the permeable area under the Zth scenario, m^2.

(3) Atmospheric Pollution Reduction

For the function of atmospheric pollution control, the values of the different LID facilities are mainly achieved through the discharge of SO_2 and the abatement of dust, without distinguishing between vegetation and grass.

$$APR_Z^{ASO_2} = S_Z^G * Q_{SO_2} * SO_{2_{Price}} \tag{14}$$

$$APR_Z^{SD} = S_Z^G * D_{Price} * F_H \tag{15}$$

$$APR_Z = APR_Z^{ASO_2} + APR_Z^{SD} \tag{16}$$

where APR_Z represents the total value of atmospheric pollution reduction under the Zth scenario, CNY; $APR_Z^{ASO_2}$ and APR_Z^{SD} are the ESV of SO_2 absorption and dust reduction by LID facilities under the Zth scenario, respectively, CNY; Q_{SO_2} represents the amount of SO_2 absorbed by plants per unit area, kg/(hm^2*a); $SO_{2_{Price}}$ represents the price of SO_2 emission, CNY/t; Q_d represents the amount of dust disposed by plants per unit area, t/(hm^2*a); D_{Price} represents the price for dust disposal, CNY/t; S_Z^G represents the area of green space under the Zth scenario, hm^2; and Q_{SO_2}, $SO_{2_{Price}}$, D_{Price}, and F_H are taken as 140.62 kg/(hm^2*a), 600 CNY/t, 10.90 t/(hm^2*a), and 150 CNY/t, respectively (Sun, 2020).

(4) Sound Absorption and Noise Reduction

In such value of ecosystem services, we discounted the value of acoustic walls for the forest strips involved in some of the LID facilities (Ma et al., 2018).

$$SA_Z = \sqrt{S_{Price} * D_{SA}} \tag{17}$$

where SA_Z is the noise reduction savings under the Zth scenario, CNY; S_{Price} is the price of the soundproof wall, taken as 425 CNY/m; and D_{SA} is the distance from the tree area converted to the noise wall, m. As there exist trees only in the LID facility type of RG, other facilities do not have the value of sound absorption and noise reduction. Since only trees in rain gardens are likely to form noise walls, other single LID paving scenarios are not considered to have the function.

2.4.2. Optimal variables and restraints

The optimization variable is the percentage of the area of the subcatchment where LID facilities are laid. The construction area of each LID facility in the study area should fluctuate within the maximum value of the corresponding subsurface area. Thus, the contstraint limits are obtained as follows:

$$A_{kmin}^m < s_k^m < A_{kmax}^m \tag{18}$$

where A^m_{kmin} and A^m_{kmin} are the minimum and maximum values of the area of the mth LID type that can be set in the kth subcatchment, respectively. In the study, A^m_{kmin} is 0 that without the pavement of LID facility and A^m_{kmin} is the area of the kth subcatchment.

2.4.3. Optimization algorithm

In this study, one of the important branches of evolutionary algorithms, i.e., the NSGA-II algorithm of genetic algorithms, is selected for incorporation into the coupled model. Coding, initial population, evaluation of fitness, selection, cross mutation, and termination rules are the key elements in genetic algorithms. Based on the MATLAB platform, the study obtained the surface runoff and pollutant load outputs from the SWMM to calculate RRR and PCR. Moreover, incorporate the cost and ESV into the NSGA-II. Specifically, the NSGA-II algorithm is first called in MATLAB to set four objective functions and four decision variables. The SWMM model is continuously called through input decision variables, after rainfall and stormwater network simulation. The output water quantity and quality results are returned to calculate the function values of runoff reduction rate and pollutant control rate, which are fed back to the objective evaluation stage in the optimization algorithm. Ultimately, the multiobjective optimization model will output the optimization solution, such as the corresponding paving ratios for each LID facility available in the case area, and the values of the four objective functions in the optimization solution. The number of iterations is 100, the population size is 50, and the decision variables take values ranging from 0 to 1.

Based on the set of Pareto frontier solutions obtained by the coupled optimization algorithm, we used the IBM SPSS Statistics software to perform an individual case rank sorting of the four objectives to obtain a reference optimum.

3. Results

3.1. Deterministic scenario analysis

The hydrological and water quality continuity errors of all scenarios were generally limited to less than 10 %, thus implying that all these scenarios can reflect the actual runoff process reasonably well so that the results are credible.

3.1.1. Surface runoff reduction

The runoff reduction performance of the six scenarios is evaluated based on the rainfall types designed for different return periods (Fig. 2).

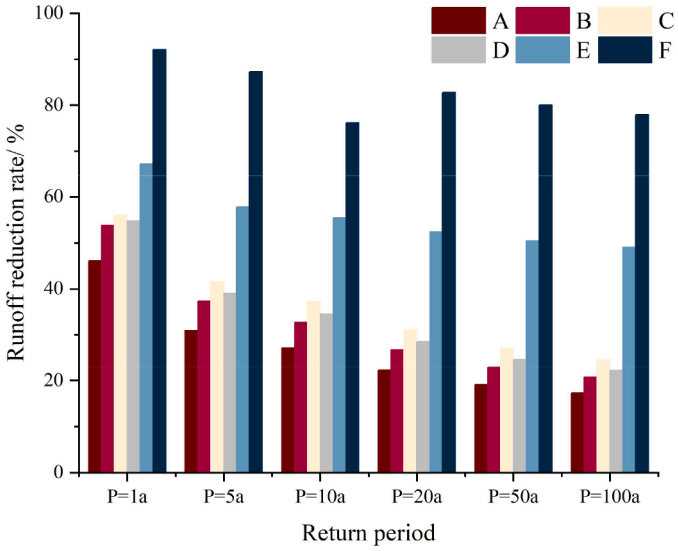

Fig. 2. Runoff reduction rate for different scenarios in different return periods.

Compared with the baseline scenario A, the remaining five scenarios all improved their runoff reduction capacity by 46.03 % to 60.87 %. The order of magnitude of RRR for the five LID paving scenarios remained constant, with the best to worst scenarios being the Scenarios F, E, C, D, and B. The integrated adjustment scenario had the highest runoff reduction of 57.17 % over the single LID paving scenario among all return periods. Moreover, compared with the baseline Scenario A, the Scenario F also had the highest of 60.87 % over it among all return periods.

As the return period increased, the RRR degree decreased for all the scenarios except Scenario F. Such decrease in RRR had the highest change value between the 1a and 5a, with average of 14.25 %. The average RRR change value of the rest four scenarios was only 3.64 %. In other words, the performance of a single LID facility for small rainfall is significantly effective than that of medium and large rainfall. After the configuration of different types of LID facilities, the ability of Scenario F to manage stormwater flooding becomes more stable and the level of volatility decreases. Although the lowest point of RRR for Scenario F is at 10a, the corresponding value is still the highest.

Scenario E is the best choice among the scenarios with a single LID facility. The variance of runoff reduction rates expanded with increasing return period of the storm for scenarios except for Scenario F.

3.1.2. Water pollution control

In terms of pollution control, PCR of the three pollutants, namely, COD, TP, and TN, gradually increased with increasing return period under different deterministic scenarios. The order of PCR remained as Scenario B < Scenario D < Scenario C < Scenario E < Scenario F (Fig. 3). Their average pollution control rates were 5.97 %, 10.82 %, 11.81 %, 59.60 %, and 88.74 %, respectively. For all the return periods, the scenarios exhibited a relative stable but a general downward trend in PCR for different pollution types and totals. It is worth pointing out that such a decline is very modest, with fluctuation frequencies ranging from 0.02 % to 4.74 % (variance of the set of declining values is 0.01 %). In addition, particularly, Scenario E had the highest control rate at P = 5a when confronted with the removal of TP and TN.

3.1.3. ESV calculation

The ESV accompanying individual LID facilities and corresponding different paving scenarios was calculated in addition to the utility of LID facilities for runoff reduction and water quality pollution control. This section further analyzes and compares the values of net carbon sink, temperature regulation, atmospheric pollution control, and noise absorption in the deterministic scenarios (Table 2). Combining the different ESV calculated for each scenario in the previous section, the Scenario D has the highest total ESV over the operational period (146,965 CNY).

3.1.3.1. Net carbon sink. For carbon sink, the benefits of Scenario F are enormous, followed by Scenarios D, E, B, and C (Fig. S6). In comparison, Scenario F also disposed the most carbon emissions, while Scenario C disposed few carbon emissions. After the calculation of the net carbon sink and the monetary conversion of CO_2, Scenario D has the highest net carbon sink value (125,981 CNY) and Scenario E has the lowest (−186,950 CNY).

3.1.3.2. Temperature regulation. For temperature regulation functions, the value of various LID facilities is mainly realized through evapotranspiration from improved water permeability. Therefore, in a rough estimate, the value of Scenarios C and D of the same size is approximately the same (12,023 CNY). Scenario F has the highest temperature regulation value (98,886 CNY), while Scenario B has the lowest (6360 CNY).

3.1.3.3. Atmospheric pollution control. Scenario F has highest value

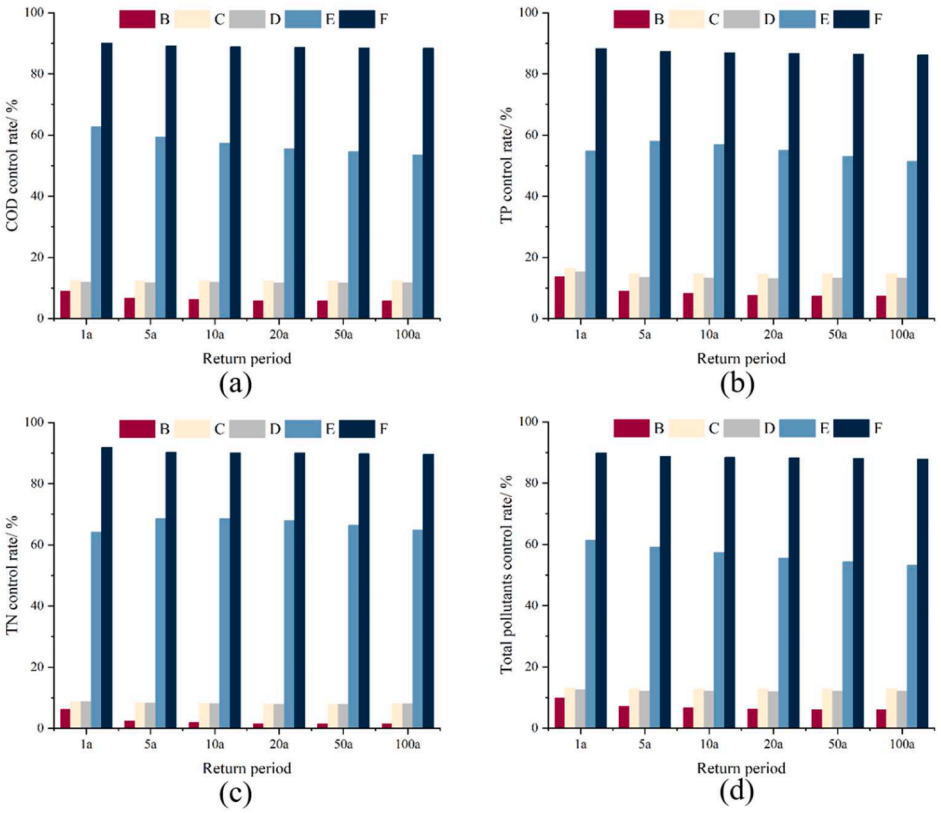

Fig. 3. Water pollution control rate for five scenarios in different return periods. (a) COD, (b) TP, (c) TN, (d) total pollutants.

Table 2
ESV for different deterministic scenarios (unit: CNY).

Scenario	Net carbon sink	Temperature regulation	Atmosphere pollution control	Noise absorption
B	9, 792	6, 360	1, 225	—
C	7, 170	12, 023	2, 316	—
D	125, 981	12, 023	2, 316	6, 646
E	−186, 950	80, 503	—	—
F	−152, 217	98, 886	3, 541	4, 131

(3541 CNY), while Scenario B has lowest (1225 CNY).

3.1.3.4. Noise absorption and reduction. Tree allotments and cover weaken noise reduction. The preliminary estimate of noise absorption and reduction value of Scenario D is 6646 CNY.

3.1.4. Cost

In terms of construction and maintenance costs for deterministic scenarios (Table S6), Scenario F has the highest construction cost (14.36×10^6 CNY) and management and maintenance cost (69.21×10^6 CNY). In reverse, Scenario B requires the lowest construction cost of 1.41×10^6 CNY and Scenario C requires the lowest management and maintenance cost of 1.94×10^6 CNY. Table S7 shows the cost of the single

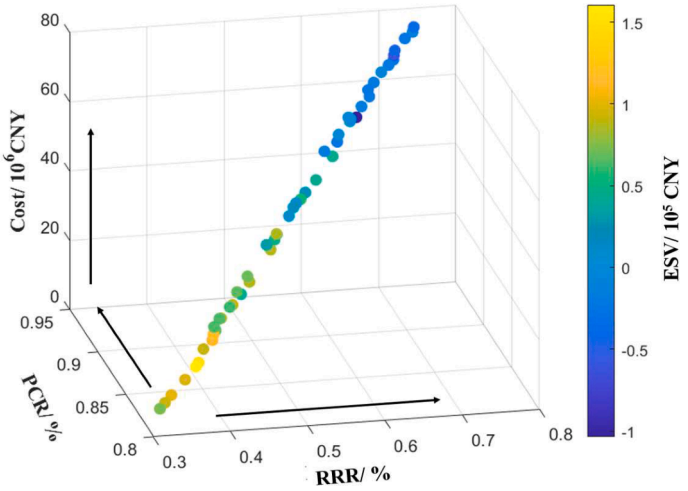

Fig. 4. Pareto frontiers under potential optimization solution.

LID facility.

3.2. Optimizing scenario analysis

3.2.1. Optimal solutions

The coupled algorithm yields a series of optimized laying schemes for LID oriented to four objectives (Fig. 4).

Higher cost for various scenarios of optimized solution improves the runoff reduction rate and pollution control rate, and the change in RRR is more acute, i.e., sensitive. There exists a trade-off between RRR and PCR. This indicates that any improvement in the objectives is at the expense of other objectives and the decision-maker can select the most suitable option according to a certain objective orientation. For example, when oriented to control the negative impacts of waterlogging, runoff, and pollution control can be achieved by investing higher costs and at the loss of ESV. The value of ecosystem services can generally be realized as positive when the cost is lower than 55.41×10^6 CNY. Besides cost, the decrease of both RRR and PCR tends to bring higher ESV. In fact, even the optimized scenario of integrated adjusted paving has limited control of runoff reduction and water quality pollution to a full percentage. Compared with deterministic paving scenarios, the recommended scenarios resulting from objective optimization are often capable of accommodating multiple requirements while satisfying different goal-oriented choices, providing options for trade-offs between conflicting relationships among the objectives.

To identify the proportion of paving relationships between each type of LID and the achievement of corresponding objective functions under different optimization scenarios, this paper used parallel plots for further comparisons as is shown in Fig. S7. In most cases, when comparing the percentages of different LID facilities paved in the optimized scenarios, higher rates of runoff reduction and water quality pollution control tend to require a greater proportion of permeable paving and vegetation swale to be installed. If a high percentage of rain gardens is selected for these two indicators, a correspondingly low percentage of green roofs will be installed. Furthermore, the converse is also applicable. Similarly, if aiming for a higher value of ecosystem services in the optimized scenario, a higher proportion of rain garden facilities tends to be selected. In terms of cost, higher expenditures are incurred due to the increased laying ratios of the LID facilities. However, these combinations tend to feature very high proportions of permeable paving and sunken green spaces (>80 %).

3.2.2. Optimization layout for preference

Even though policymakers can choose preferred paving options based on different goal orientations, the study offers a relatively optimal scheme for preference based on the individual case rank shown in Table S8.

The solution prioritizes RG that can be attributed to the high ESV. It allocates little proportion for PP at the compensation of good performance in runoff reduction and water pollution control. Moreover, the optimal scheme assigns 14.25 % and 13.86 % for GR and VS, respectively, considering their poor performance on each objective during the deterministic scenario analysis. In comparison, Scenario F achieves a runoff reduction of 87.23 % at the $P = 5$a event. After optimization as the paving ratio especially PP drastically decreases, the runoff reduction rate reaches only 32.48 %. However, the PCR of the optimal scheme reaches 82.22 % slightly lower than 88.77 % of Scenario F. This implies that the change in the paving ratio has a greater impact on the runoff reduction rate, while a combination of LID facilities can be effective in improving water quality pollution. The optimal scenario required the lowest cost input of 2.29×10^6 CNY but was able to realize about 0.73×10^5 CNY in ESV.

4. Discussion

4.1. Utility of LID facilities

LID facilities do enhance a community's capacity to adapt to diverse stormwater scenarios, and this type of paving may be an effective tool. In this study, six different LID deterministic scenarios were designed to identify the intrinsic mechanisms and characteristics of different LID facility functions that work through deterministic analysis. The runoff reduction and water quality pollution control for the LID facilities decreased to varying degrees as the return period increased. Moreover, Zhang et al. (2019) demonstrated that the runoff reduction efficiency of LID facility paving decreases with increasing storm return period. However, such an effect is not significant for peak time occurrence. Among the individual LID deterministic scenarios, Scenario B has the worst performance in terms of RRR and PCR, which may be due to the small area of green roofs laid, and the fact that the green roofs are based on the buildings in the neighborhood, which are scattered with high fragmentation and poor connectivity. Scenario E is far superior in both RRR and PCR. This reflects the importance of permeability to this study area, although LIDs that performed optimally in other studies differed. The decrease in nutrient loading was also substantial, which was attributed to the infiltration increase and runoff decrease caused by the porous pavement. Martin et al. (2015) study showed that the addition of porous pavement to a parking lot was able to contribute to a decrease in mean annual runoff of up to 24 %. Yet such simulation results may not imply the suitability of permeable paving for any region. Different land uses and building densities are associated with widely different preferences for LID facilities (Chen, 2015). For example, Suresh et al. (2023) revealed the highest percentage reduction in runoff characteristics for green roofs through four microwatersheds in Northeast India under climate change simulations, while Peng et al. (2020) found that vegetated depressions are more effective than green roofs in reducing overflow water depth. These seemingly paradoxical results may also illustrate the universality of LID facilities for stormwater control and the discrepancy of different LID facilities functioning in different areas.

The study organically grouped the four LIDs and found that the integrated scenarios performed well in terms of both water quantity and quality results. By comparing runoff changes from the 1a to 100a return period, the study found that the single paving scenarios tended to lose their ability to control rainfall dramatically after the 5a return period. Nevertheless, the integrated scenario enhanced the effectiveness of the facility in controlling heavy rainfall runoff while maintaining a higher reduction rate. The runoff control capability of Scenario F is always much higher than the LID single paving scenario. It may be more sensitive to the frequency and intensity of storms in 10a and lead to its worst performance in the RRR. The RRR performance of Scenario F remains at a higher level as the intensity of the storm increases.

It is worth mentioning that a mix of all facilities may not be necessary for the actual laying of LID facilities. For example, Hua et al. (2020) found that a combination of bioretention, infiltration trenches, and rain barrels in the city center of Chaohu, Anhui, China, performed the best control.

Of all the paving scenarios, the rain garden scenario showed the highest performance in terms of ecosystem services. Consistent with the results mirrored in the scenario modeling for this study, the adoption of LID within community gardens is most conducive to the provision of diverse ecosystem services (Evans et al., 2022). In addition, it is essential to recognize the multifunctionality of LID, as concentrating solely on one benefit can lead to negative consequences from other perspectives, despite the multiple benefits it provides for cities (Demuzere et al., 2014). Although the potential for carbon storage in vegetation of LID facilities is substantial, few consideration has been given to the carbon emissions from the raw materials, construction, and maintenance of the facilities (Chen, 2015). In our study, the establishment of permeable paving can result in significant carbon emissions, adding pressure to the

environment. LID facilities can reduce air and surface temperatures through shading and evapotranspiration, an effective form of cooling. The study mainly considered the cooling effect of the facility through evaporative heat absorption by the permeable surface. It was found that the cooling effect of Scenario E was much higher than the other single LID paved scenarios. If the use of trees is considered, the cooling effectiveness of LID settings that include vegetation may be improved. Erlwein et al. (2021) illustrated that newly planted trees only slightly improved daytime thermal comfort. It may imply that the utility of LID facilities for cooling needs to be accounted for over a longer operating period. Different facilities have different cooling capacities, while reasonable vegetation composition and LID combinations can improve cooling performance (Cavan et al., 2014; Marando et al., 2019). Xi et al. (2022) also demonstrated that the combination of green roofs and other facilities provided better cooling than the facilities alone. The estimated value per unit area of removal of air pollutants by green spaces in this study is slightly lower than the results of She et al. (2021). It appears that their differentiation can be made in the future by the effect of the arrangement of different facilities in various locations. A further study considered PM_{10}, $PM_{2.5,}$ and other pollutants (SO_2, $NO_{2,}$ and CO_2) more comprehensive than the dust and SO_2 considered in this paper. Aspects such as the location, shape, and meteorological conditions of the area can affect the functioning of LID facilities (Tomson et al., 2021). Green roofs and rain gardens can significantly reduce noise through the high absorption coefficient of the vegetation layer. Green roofs based on low buildings may have less sound absorption and noise reduction capacity than green roofs on taller buildings, giving the potential to distinguish the effect of building height on fine-tuning sound absorption.

Overall, the low value of ecosystem services estimated for LID facilities in this study can be traced to the following aspects. Rain gardens and green space establishments in a community may provide space for residents to spend their leisure time and offer many other health-enhancing benefits (Markevych et al., 2017). The study may underestimate the ESV of LID facilities, because some types such as biodiversity are difficult to measure monetarily (Langemeyer et al., 2015). In addition, some studies have included runoff reduction, a category of flood control value, as ESV of the facility (De Valck et al., 2019). Particularly, the ESV in the studies are much smaller than the cost. In fact, when LID facility layouts are incorporated into community planning, residents are willing to pay a fee for the welfare they receive (Chen et al., 2020). When casting future research on larger scales, it is even more necessary to consider the value of LID facilities for biodiversity, human well-being, etc. Accordingly, such an evaluation framework can be used in turn to improve and optimize the original solution.

4.2. Grouping of LID facilities for optimal configuration

In the process of comprehensively weighing the four objectives to obtain the optimal laying ratio, it is necessary to search the optimal unique solution for reference. Wang, M. et al. (2023) set up different configuration scenarios based on the characteristics of the gray-green infrastructure and optimized to obtain the optimal configuration of the scenarios, comparing with the scenarios of the completely gray infrastructure. In the case of practical planning of community layout, it may be essential to achieve higher runoff reduction and water quality pollution control capacity. Therefore, more weight can be appropriately assigned to RRR and PCR when sorting to select the optimal solution. Although all aspects are considered, a reduction in costs and an increase in ESV will inevitably lead to a decrease in RRR and PCR. Meanwhile, a larger ESV can only be realized when the cost function is within a certain range. Once the costs are prohibitive, ESV is also substantially reduced. Moreover, PCR is much less sensitive to the paving ratio than RRR. This may be due to the higher requirements of RRR on the location and continuity of LID facility laying, etc., while PCR requires the presence of LID facilities more to intervene in the formation of surface source pollution. To be admitted, this study regarded the importance of all objectives as the same, thus ignoring the differences in the weights of the objectives under various goal orientations. Decision-makers can optimize and select according to the actual goal needs and assign greater weight values to the more preferred goals. For example, Wang, J. et al. (2023) partitioned the area functionally and differentiated the objectives to be achieved in different partitions before optimization. Zhu et al. (2023) selected the optimal layout plan according to the preference of different objectives.

It is worth noting that the study found some conflicts and trade-offs between RRR, PCR, cost, and ESV. When the sponge city program aims to reduce the risk for areas with high risk of flooding, it is logical to focus more on RRR and PCR and lose some ESV by increasing the cost inputs. An improvement of RRR means a massive increase in the proportion of PP, whereas an increase in PCR only requires a reasonable mix of different LID facilities. In contrast, if it is just to increase the city's ability to resist storm scenarios, loosening some of the RRR and PCR requirements may increase the ESV at the appropriate cost simultaneously. It was difficult to reconcile ESV and cost. For example, the priority given to the laying of RG is beneficial in terms of increasing ESV; however, it implies a drastic increase in cost.

5. Conclusion

This study optimized LID facilities by coupling SWMM and NSGA-II, considering ESV of the LID facilities. ESV such as net carbon sink, temperature regulation, air pollution control, and sound absorption and noise reduction were monetized. Moreover, this study then used SWMM to simulate and identify LID facility layout scenarios with different configurations, exploring differences in the response relationships of LID facilities to different targets. Further, based on the deterministic scenario, SWMM and NSGA-II were coupled to solve for the optimal layout ratio with the four optimization objectives such as maximum runoff reduction rate, maximum water quality pollution control rate, minimum cost input, and maximum ESV. Take a neighborhood in Beijing, China, as an example.

It was found that grouping and planning single type LID facilities under different return periods can improve both runoff reduction rates and water quality pollution control by more than 20 % and enhance the effectiveness of the facilities in controlling heavy rainfall runoff. However, the magnitude of the decreasing trend in the removal rates of COD, TP, and TN pollutants was minor for the different scenarios. As for the ESV and cost, during the operation period, the carbon emissions from permeable paving are much higher than the carbon sinks that require monetary compensation. Instead, the rain garden scenario provides nearly 1.5×10^5 CNY in ESV. In addition, green roofs have the highest total cost per unit area of LID facilities.

Finally, the study obtained the optimal allocation ratios of LID facilities in the Scenario F under the $P = 5$a return period, where an increase in runoff reduction rate leads to a weakness in water quality pollution control. As cost increases, runoff reduction rate and water quality pollution control rate will improve, and the former changes are more sensitive and vigorous. The value of ecosystem services tends to be realized as a net benefit when the cost input is less than 55.41×10^6 CNY. When weighing the four objectives collectively, the optimal solution provides a runoff reduction rate and a pollution control rate of 32.4 % and 82.22 %, respectively. It requires a cost input of 2.29×10^6 CNY and achieves a total ESV of about 0.73×10^5 CNY. The coupled model can provide alternative optimization solutions if the decision-maker oriented to one or more other objectives.

The corresponding innovations of this study are summarized as follows: (1) to introduce ESV accompanying LID facilities for constructing a more complete objective optimization framework, (2) to explore the response and contribution of LID facilities to different objectives under multiple rainfall scenarios, and (3) to realize the optimization of the layout of LID facilities with the consideration of the performances of each kind of LID facility that are identified via the deterministic

scenarios.

The study is cursory about cost and ESV accounting for LID facilities, but the proposed framework can provide ideas for optimal configuration. Further research is necessary to deeply explore the coupled synergistic mechanisms of LID facilities and gray infrastructure at different scales, combinations of deployment locations, and in various stages of rainfall in the future.

CRediT authorship contribution statement

Xuanyi Jin: Writing – original draft, Methodology, Investigation, Formal analysis, Data curation. **Delin Fang:** Writing – review & editing, Validation, Project administration, Funding acquisition, Conceptualization. **Bin Chen:** Validation, Project administration, Funding acquisition, Conceptualization. **Hao Wang:** Validation, Data curation, Conceptualization.

Declaration of competing interest

The authors declare that they have no known competing financial interests or personal relationships that could have appeared to influence the work reported in this paper.

Data availability

Data will be made available on request.

Acknowledgement

This work was supported by the National Natural Science Foundation of China (No. 72174029, 72091511), Project Supported by State Key Laboratory of Earth Surface Processes and Resource Ecology (Project Number 2022-ZD-04), the Fundamental Research Funds for the Central Universities.

Supplementary materials

Supplementary material associated with this article can be found, in the online version, at doi:10.1016/j.resconrec.2024.107794.

References

Alamdari, N., Sample, D.J., 2019. A multiobjective simulation-optimization tool for assisting in urban watershed restoration planning. J. Clean Prod 213, 251–261.
Ashrafi, S., Kerachian, R., Pourmoghim, P., Behboudian, M., Motlaghzadeh, K., 2022. Evaluating and improving the sustainability of ecosystem services in river basins under climate change. Sci. Total Environ. 806, 150702.
Behboudian, M., Kerachian, R., Motlaghzadeh, K., Ashrafi, S., 2021. Evaluating water resources management scenarios considering the hierarchical structure of decision-makers and ecosystem services-based criteria. Sci. Total Environ. 751, 141759.
Cavan, G., Lindley, S., Jalayer, F., Yeshitela, K., Pauleit, S., Renner, F., Gill, S., Capuano, P., Nebebe, A., Woldegerima, T., 2014. Urban morphological determinants of temperature regulating ecosystem services in two African cities. Ecol. Indic. 42, 43–57.
Chen, S., Wang, Y., Ni, Z., Zhang, X., Xia, B., 2020. Benefits of the ecosystem services provided by urban green infrastructures: differences between perception and measurements. Urb. Fores. Urb. Green. 54, 126774.
Chen, W.Y., 2015. The role of urban green infrastructure in offsetting carbon emissions in 35 major Chinese cities: a nationwide estimate. Cities 44, 112–120.
Chuang, W., Lin, Z., Lin, T., Lo, S., Chang, C., Chiueh, P., 2023. Spatial allocation of LID practices with a water footprint approach. Sci. Total Environ. 859, 160201.
Darnthamrongkul, W., Mozingo, L.A., 2021. Toward sustainable stormwater management: understanding public appreciation and recognition of urban Low Impact Development (LID) in the San Francisco Bay Area. J. Environ. Manage. 300, 113716.
De Valck, J., Beames, A., Liekens, I., Bettens, M., Seuntjens, P., Broekx, S., 2019. Valuing urban ecosystem services in sustainable brownfield redevelopment. Ecosyst. Serv. 35, 139–149.
Demuzere, M., Orru, K., Heidrich, O., Olazabal, E., Geneletti, D., Orru, H., Bhave, A.G., Mittal, N., Feliú, E., Faehnle, M., 2014. Mitigating and adapting to climate change: multi-functional and multi-scale assessment of green urban infrastructure. J. Environ. Manage. 146, 107–115.
Deng, L., Yang, Z., Su, W., 2019. Valuing the water ecosystem service and analyzing its impact factors in Chongqing City under the background of urbanization. Res. Soil Water. Conser. 26, 208–216.
Eckart, K., McPhee, Z., Bolisetti, T., 2017. Performance and implementation of low impact development–A review. Sci. Total Environ. 607, 413–432.
Eckart, K., McPhee, Z., Bolisetti, T., 2018. Multiobjective optimization of low impact development stormwater controls. J. Hydrol. 562, 564–576.
Erlwein, S., Zölch, T., Pauleit, S., 2021. Regulating the microclimate with urban green in densifiying cities: Joint assess. two scales. Build. Environ. 205, 108233.
Eskandaripour, M., Golmohammadi, M.H., Soltaninia, S., 2023. Optimization of low-impact development facilities in urban areas using slime mould algorithm. Sustain. Cities. Soc. 93, 104508.
Evans, D.L., Falagán, N., Hardman, C., Kourmpetli, S., Liu, L., Mead, B., Davies, J., 2022. Ecosystem service delivery by urban agriculture and green infrastructure–a systematic review. Ecosyst. Serv. 54, 101405.
Gao, J., Li, J., Li, Y., Xia, J., Lv, P., 2021. A distribution optimization method of typical LID facilities for sponge city construction. Ecohydrol. Hydrobiol. 21 (1), 13–22.
Ghodsi, S.H., Zahmatkesh, Z., Goharian, E., Kerachian, R., Zhu, Z., 2020. Optimal design of low impact development practices in response to climate change. J. Hydrol 580, 124266.
Hamouz, V., Muthanna, T.M., 2019. Hydrological modelling of green and grey roofs in cold climate with the SWMM model. J. Environ. Manage. 249, 109350.
Hashemi, M., Mahjouri, N., 2022. Global sensitivity analysis-based design of low impact development practices for urban runoff management under uncertainty. Water. Res. Manag. 36 (9), 2953–2972.
Heidari, B., Prideaux, V., Jack, K., Jaber, F.H., 2023. A planning framework to mitigate localized urban stormwater inlet flooding using distributed Green Stormwater Infrastructure at an urban scale: case study of Dallas, Texas. J. Hydrol 621, 129538.
Heusinger, J., Weber, S., 2017. Extensive green roof CO2 exchange and its seasonal variation quantified by eddy covariance measurements. Sci. Total Environ. 607, 623–632.
Hou, J., Wang, X., Li, B., Gao, X., Huang, M., Han, H., Shen, R., 2021. Refined simulation method of the rainfall–runoff processes in a residential area with LID measures. J. Hydrol. Eng 26 (12), 04021038.
Hou, J., Zhu, M., Wang, Y., Sun, S., 2020. Optimal spatial priority scheme of urban LID-BMPs under different investment periods. Landsc. Urban. Plan. 202, 103858.
Hua, P., Yang, W., Qi, X., Jiang, S., Xie, J., Gu, X., Li, H., Zhang, J., Krebs, P., 2020. Evaluating the effect of urban flooding reduction strategies in response to design rainfall and low impact development. J. Clean. Prod. 242, 118515.
Huang, C., Hsu, N., Liu, H., Huang, Y., 2018. Optimization of low impact development layout designs for megacity flood mitigation. J. Hydrol. 564, 542–558.
Huang, L., Yang, H., SHE, Q., Yuan, G., 2023. Research on carbon sequestration accounting and its value analysis of mining areas in Guangxi. Environmen. Ecol. 5 (12), 61–66.
Huber, W., Dickinson, R., 1988. Storm Water Management Model User's Manual. US Environmental Protection Agency, Georgia.
Huber, W.C., Dickinson, R.E., Barnwell Jr., T.O., Branch, A., 1988. Storm Water Management model; Version 4. Environmental Protection Agency, United States.
Ji, H., Peng, D., Fan, C., Zhao, K., Gu, Y., Liang, Y., 2022. Assessing effects of non-point source pollution emission control schemes on Beijing's sub-center with a water environment model. Urb. Cli. 43, 101148.
Ji, X., Dong, W., Wang, W., Dai, X., Huang, H., 2024. impacts of climate change on extreme precipitation events and urban waterlogging: a case study of Beijing. Nat. Hazards Rev. 25 (1), 05023014.
Koc, K., Ekmekcioğlu, Ö., Özger, M., 2021. An integrated framework for the comprehensive evaluation of low impact development strategies. J. Environ. Manage. 294, 113023.
Korkou, M., Tarigan, A.K., Hanslin, H.M., 2023. The multifunctionality concept in urban green infrastructure planning: a systematic literature review. Urb. Urb. Green., 127975
Langemeyer, J., Baró, F., Roebeling, P., Gómez-Baggethun, E., 2015. Contrasting values of cultural ecosystem services in urban areas: the case of park Montjuïc in Barcelona. Ecosyst. Serv. 12, 178–186.
Li, C., Zheng, T., Peng, K., Cheng, W., Xu, J., Qiao, J., Huang, J., 2019. Study on carbon emission of sponge city stormwater system based on life cycle assessment. Environ. Sustain. Develop. 44 (01), 132–137.
Liao, Z., Zhang, G., Wu, Z., He, Y., Chen, H., 2015. Combined sewer overflow control with LID based on SWMM: an example in Shanghai, China. Water Sci. Technol. 71 (8), 1136–1142.
Liu, Y., Li, G., Zeng, P., Zhang, X., Tian, T., Feng, H., Che, Y., 2022. Challenge of rainwater harvesting in Shanghai, China: a public psychological perspective. J. Environ. Manage. 318, 115584.
Lovell, S.T., Taylor, J.R., 2013. Supplying urban ecosystem services through multifunctional green infrastructure in the United States. Landsc. Ecol 28, 1447–1463.
Luo, Z., Tian, J., Zeng, J., Pilla, F., 2023. Assessing the spatial pattern of supply-demand mismatches in ecosystem flood regulation service: a case study in Xiamen. Appl. Geogr. 160, 103113.
Ma, P., Wang, Z., Li, Q., 2018. Evaluation of forest ecosystem services in Beidaihe district of Qinhuangdao city. Bullet. Soil Water Conserv 38 (3), 286–292.
Marando, F., Salvatori, E., Sebastiani, A., Fusaro, L., Manes, F., 2019. Regulating ecosystem services and green infrastructure: assessment of urban heat island effect mitigation in the municipality of Rome, Italy. Ecol. Modell 392, 92–102.
Markevych, I., Schoierer, J., Hartig, T., Chudnovsky, A., Hystad, P., Dzhambov, A.M., De Vries, S., Triguero-Mas, M., Brauer, M., Nieuwenhuijsen, M.J., 2017. Exploring

pathways linking greenspace to health: theoretical and methodological guidance. Environ. Res. 158, 301–317.
Martin, A., Ahiablame, L., Engel, B., 2015. Modeling low impact development in two Chicago communities. Environ. Sci.: Water Res. Technol 1 (6), 855–864.
Ministry of Housing and Urban-Rural Development of the People's Republic of China. 2018. Assessment standard for sponge city construction effect. Retrieved from: https://www.mohurd.gov.cn/gongkai/zhengce/zhengcefilelib/201904/20190410_240118.html (in Chinese).
Minh Hai, D., 2020. Optimal planning of low-impact development for TSS control in the upper area of the Cau Bay River Basin. Vietnam Water 12 (2), 533.
Nash, J.E., Sutcliffe, J.V., 1970. River flow forecasting through conceptual models part I—a discussion of principles. J. Hydrol 10 (3), 282–290.
Peng, J., Zhong, X., Yu, L., Wang, Q., 2020. Simulating rainfall runoff and assessing low impact development (LID) facilities in sponge airport. Water Sci. Technol 82 (5), 918–926.
Qin, H., Li, Z.-x., Fu, G., 2013. The effects of low impact development on urban flooding under different rainfall characteristics. J. Environ. Manage. 129, 577–585.
Reckner, M., Tien, I., 2023. Community-scale spatial mapping to prioritize green and grey infrastructure locations to increase flood resilience. Sustain. Resil. Infrastruc. 8 (sup1), 289–310.
Rezaei, A.R., Ismail, Z., Niksokhan, M.H., Dayarian, M.A., Ramli, A.H., Yusoff, S., 2021. Optimal implementation of low impact development for urban stormwater quantity and quality control using multi-objective optimization. Environ. Monit. Assess 193, 1–22.
Rong, Q., Liu, Q., Yue, W., Xu, C., Su, M., 2024. Optimal design of low impact development at a community scale considering urban non-point source pollution management under uncertainty. J Clean Prod 434, 139934.
Shafique, M., Kim, R., 2017. Retrofitting the low impact development practices into developed urban areas including barriers and potential solution. Open Geosci 9 (1), 240–254.
She, L., Wei, M., You, X., 2021. Multi-objective layout optimization for sponge city by annealing algorithm and its environmental benefits analysis. Sustain. Cities Soc. 66, 102706.
Shojaeizadeh, A., Geza, M., Hogue, T.S., 2021. GIP-SWMM: a new green infrastructure placement tool coupled with SWMM. J. Environ. Manage. 277, 111409.
Song, J., Chung, E., Kim, S., 2018. Decision support system for the design and planning of low-impact development practices: the case of Seoul. Water (Basel) 10 (2), 146.
Sun, W., 2020. Quantitative and Comprehensivee Valuation of the Benefits of Sponge Cityc On Struction——Taking Guyuan Ningxia as An Example. Xi'an University of Technology.
Suresh, A., Pekkat, S., Subbiah, S., 2023. Quantifying the efficacy of low impact developments (LIDs) for flood reduction in micro-urban watersheds incorporating climate change. Sustain. Cities Soc. 95, 104601.
Toledo-Gallegos, V.M., My, N.H., Tuan, T.H., Börger, T., 2022. Valuing ecosystem services and disservices of blue/green infrastructure. Evidence from a choice experiment in Vietnam. Econ. Anal. Pol 75, 114–128.
Tomson, M., Kumar, P., Barwise, Y., Perez, P., Forehead, H., French, K., Morawska, L., Watts, J.F., 2021. Green infrastructure for air quality improvement in street canyons. Environ. Int 146, 106288.
Truong, S., Gray, T., Ward, K., 2022. Enhancing urban nature and place-making in social housing through community gardening. Urb. Fores. Urb. Green 72, 127586.
Van Oijstaeijen, W., e Silva, M.F., Back, P., Collins, A., Verheyen, K., De Beelde, R., Cools, J., Van Passel, S., 2023. The Nature Smart Cities business model: a rapid decision-support and scenario analysis tool to reveal the multi-benefits of green infrastructure investments. Urb. Fores. Urb. Green 84, 127923.
Wang, J., Liu, J., Yang, Z., Mei, C., Wang, H., Zhang, D., 2023a. Green infrastructure optimization considering spatial functional zoning in urban stormwater management. J. Environ. Manage. 344, 118407.
Wang, M., Liu, M., Zhang, D., Qi, J., Fu, W., Zhang, Y., Rao, Q., Bakhshipour, A.E., Tan, S. K., 2023b. Assessing and optimizing the hydrological performance of Grey-Green infrastructure systems in response to climate change and non-stationary time series. Water Res. 232, 119720.
Wang, R., Brent, D., Wu, H., 2022a. Willingness to pay for ecosystem benefits of green stormwater infrastructure in Chinese sponge cities. J. Clean Prod 371, 133462.
Wang, W., Deng, X., Wang, Y., Peng, L., Yu, Z., 2022b. Impacts of infrastructure construction on ecosystem services in new-type urbanization area of North China Plain. Resour., Conservat. Recycl 185, 106376.
Xi, C., Ding, J., Wang, J., Feng, Z., Cao, S., 2022. Nature-based solution of greenery configuration design by comprehensive benefit evaluation of microclimate environment and carbon sequestration. Ener. Build 270, 112264.
Yang, B., Zhang, T., Li, J., Feng, P., Miao, Y., 2023. Optimal designs of LID based on LID experiments and SWMM for a small-scale community in Tianjin, north China. J. Environ. Manage. 334, 117442.
Yin, D., Evans, B., Wang, Q., Chen, Z., Jia, H., Chen, A.S., Fu, G., Ahmad, S., Leng, L., 2020. Integrated 1D and 2D model for better assessing runoff quantity control of low impact development facilities on community scale. Sci. Total Environ 720, 137630.
Yu, Y., Zhou, Y., Guo, Z., van Duin, B., Zhang, W., 2022. A new LID spatial allocation optimization system at neighborhood scale: integrated SWMM with PICEA-g using MATLAB as the platform. Sci. Total Environ 831, 154843.
Zhai, J., Ren, J., Xi, M., Tang, X., Zhang, Y., 2021. Multiscale watershed landscape infrastructure: integrated system design for sponge city development. Urb. Fores. Urb. Green 60, 127060.
Zhang, J., Zhang, Y., Sun, S., Zhang, W., Zhang, S., 2019. Analysis of the effect of low impact development on urban runoff control based on the SWMM model. J. Coast. Res 96 (SI), 62–67.
Zhang, K., Chui, T.F.M., Yang, Y., 2018. Simulating the hydrological performance of low impact development in shallow groundwater via a modified SWMM. J. Hydrol 566, 313–331.
Zhang, S., 2012. Stormwater Management Program Simulation Study On a Residential Area in Beijing. Beijing Institute of Architecture and Engineering, Beijing.
Zhang, Y., Yang, F., He, Y., Wang, K., 2021. The 'Sponge City' construction of Zhoushan city based on analysis of water ecosystem services value. Ocean Developm. Manage. 10, 45–51.
Zhi, X., Chen, L., Shen, Z., 2018. Impacts of urbanization on regional nonpoint source pollution: case study for Beijing, China. Environ. Sci. Pollut. Res 25, 9849–9860.
Zhu, Y., Xu, C., Liu, Z., Yin, D., Jia, H., Guan, Y., 2023. Spatial layout optimization of green infrastructure based on life-cycle multi-objective optimization algorithm and SWMM model. Resour., Conservat. Recycl 191, 106906.